New Journal of Chemistry

Syntheses and characterization of monobasic tridentate Cu(II) Schiff-base complexes for efficient oxidation of 3,5-di-*tert*-butylcatechol and oxidative bromination of organic substrates.

Sweta Kumari[a], Arun Kumar Mahato[a], Abhishek Maurya[a], Vijay Kumar Singh[a], Neha Keshwarwani[a], Payal Kachhap[a], Igor Koshevoy[b], Chanchal Haldar[a]*

Supplementary Information's

Table S1: Single crystal X-ray crystallographic bond length and bond angle for complex **1**

Bond Distance (Å)		Bond Angle (°)	
C(1)-O(1)	1.3244(18)	C(7)-N(1)-C(8)	118.18(13)
C(4)-C(5)	1.372(3)	C(7)-N(1)-Cu(1)	126.83(11)
C(4)-H(4)	0.9500	C(8)-N(1)-Cu(1)	114.99(9)
C(5)-C(6)	1.412(2)	C(10)-N(2)-C(13)	107.23(11)
C(5)-H(5)	0.9500	C(10)-N(2)-C(9)	110.76(12)
C(6)-C(7)	1.433(2)	C(13)-N(2)-C(9)	113.34(11)
C(7)-N(1)	1.2843(19)	C(10)-N(2)-Cu(1)	114.09(8)
C(7)-H(7)	0.9500	C(13)-N(2)-Cu(1)	107.84(9)
C(8)-N(1)	1.463(2)	C(9)-N(2)-Cu(1)	103.67(8)
C(8)-C(9)	1.509(2)	C(12)-N(3)-C(11)	112.77(11)
C(8)-H(8A)	0.9900	C(12)-N(3)-H(3N1)	109.2
C(8)-H(8B)	0.9900	C(11)-N(3)-H(3N1)	104.9
C(9)-N(2)	1.4936(18)	C(12)-N(3)-H(3N2)	109.0
C(9)-H(9A)	0.9900	C(11)-N(3)-H(3N2)	110.1
C(9)-H(9B)	0.9900	H(3N1)-N(3)-H(3N2)	110.8
C(10)-N(2)	1.4821(19)	C(20)-N(4)-C(21)	118.52(13)
C(10)-C(11)	1.518(2)	C(20)-N(4)-Cu(2)	126.90(10)
C(10)-H(10A)	0.9900	C(21)-N(4)-Cu(2)	114.54(10)
C(10)-H(10B)	0.9900	C(26)-N(5)-C(23)	107.23(12)
C(11)-N(3)	1.491(2)	C(26)-N(5)-C(22)	111.02(12)
C(11)-H(11A)	0.9900	C(23)-N(5)-C(22)	113.56(12)
C(11)-H(11B)	0.9900	C(26)-N(5)-Cu(2)	114.30(9)
C(12)-N(3)	1.487(2)	C(23)-N(5)-Cu(2)	107.57(9)
C(12)-C(13)	1.518(2)	C(22)-N(5)-Cu(2)	103.26(8)
C(13)-N(2)	1.4892(18)	C(24)-N(6)-C(25)	112.47(12)
C(13)-H(13A)	0.9900	C(24)-N(6)-H(6N1)	111.2
C(13)-H(13B)	0.9900	C(25)-N(6)-H(6N1)	105.4
C(14)-O(2)	1.3286(17)	C(24)-N(6)-H(6N2)	108.2
C(14)-C(15)	1.408(2)	C(25)-N(6)-H(6N2)	109.6
C(14)-C(19)	1.415(2)	H(6N1)-N(6)-H(6N2)	110.0
C(24)-H(24B)	0.9900	C(1)-O(1)-Cu(1)	127.50(10)

C(25)-N(6)	1.498(2)	C(14)-O(2)-Cu(2)	127.19(9)
C(25)-C(26)	1.519(2)	O(1)-Cu(1)-N(1)	92.71(5)
C(25)-H(25A)	0.9900	O(1)-Cu(1)-N(2)	174.24(5)
C(25)-H(25B)	0.9900	N(1)-Cu(1)-N(2)	83.71(5)
C(26)-N(5)	1.487(2)	O(1)-Cu(1)-Cl(1)	89.05(4)
C(26)-H(26A)	0.9900	N(1)-Cu(1)-Cl(1)	158.14(4)
C(26)-H(26B)	0.9900	N(2)-Cu(1)-Cl(1)	92.60(3)
N(1)-Cu(1)	1.9449(12)	O(1)-Cu(1)-Cl(2)	91.92(4)
N(2)-Cu(1)	2.0885(12)	N(1)-Cu(1)-Cl(2)	98.74(4)
N(3)-H(3N1)	0.8096	N(2)-Cu(1)-Cl(2)	93.09(4)
N(3)-H(3N2)	0.8598	Cl(1)-Cu(1)-Cl(2)	102.982(15)
N(4)-Cu(2)	1.9541(12)	O(2)-Cu(2)-N(4)	92.45(5)
N(5)-Cu(2)	2.0840(12)	O(2)-Cu(2)-N(5)	174.09(5)
N(6)-H(6N1)	0.8356	N(4)-Cu(2)-N(5)	83.64(5)
N(6)-H(6N2)	0.8797	O(2)-Cu(2)-Cl(3)	88.93(3)
O(1)-Cu(1)	1.9272(11)	N(4)-Cu(2)-Cl(3)	158.25(4)
O(2)-Cu(2)	1.9358(10)	N(5)-Cu(2)-Cl(3)	93.08(3)
Cu(1)-Cl(1)	2.2980(4)	O(2)-Cu(2)-Cl(4)	91.84(4)
Cu(1)-Cl(2)	2.6942(5)	N(4)-Cu(2)-Cl(4)	99.26(4)
Cu(2)-Cl(3)	2.2894(4)	N(5)-Cu(2)-Cl(4)	93.16(4)
Cu(2)-Cl(4)	2.6636(5)	Cl(3)-Cu(2)-Cl(4)	102.388(16)

Table S2: Selected FTIR stretching frequencies for the ligands and complexes.

Compound	$\nu_{(O-H)}$	$\nu_{(N-H)}$	$\nu_{(C-O)}$	$\nu_{(C=N)}$	$\nu_{(N-H)wagging}$
[Hsal-ppz] (I)	3369	2928	1279	1635	759
[Hyap-ppz] (II)	3432	2929	1299	1615	755
[Cu(sal-ppzH)Cl_2] (**1**)	3435	2945	1201	1600	754
[Cu(hyap-ppzH)Cl_2] (**2**)	3413	2926	1233	1601	764
PS-[Cu (sal-ppzH)Cl_2] (**3**)	3366	2916	1362	1598	756
PS-[Cu (hyap-ppzH)Cl_2] (**4**)	-	2916	1366	1601	756

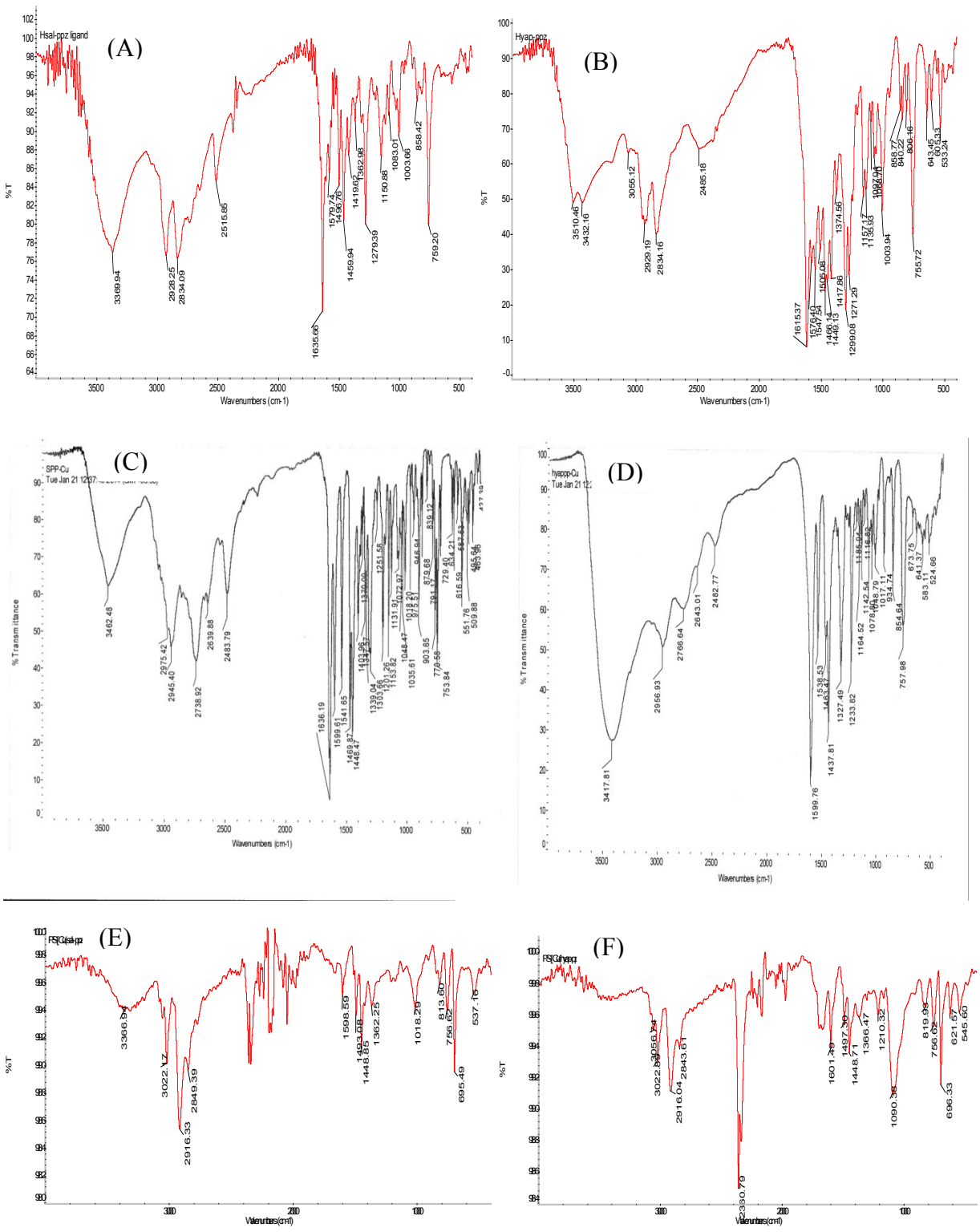

Figure S1: IR spectra of (A) [Hsal-ppz] (**I**); (B) [Hyap-ppz] (**II**); (C) [Cu^{II}(sal-ppzH)Cl_2] (**1**); (D) [Cu^{II}(hyap-ppzH)Cl_2] (**2**); (E) PS-[Cu^{II}(sal-ppzH)Cl_2] (**3**); (F) PS-[Cu^{II}(hyap-ppzH)Cl_2] (**4**).

Table S3: Selected UV-Visible absorption data for the ligands and copper (II) complexes.

Compound	Solvent	λ_{max}(nm)/ ε(litre mol^{-1} cm^{-1})
[Hsal-ppz] ***(I)***	MeOH	254(1.114×10^4), 272(5.726×10^3), 316(3.609×10^3), 405(1.460×10^3)
[Hyap-ppz] ***(II)***	MeOH	270 (7.5138×10^3), 324(1.936×10^3), 388(3.508×10^3)
$[Cu^{II}(sal\text{-}ppzH)Cl_2]$ (**1**)	MeOH	225(2.170×10^3), 238(2.126×10^3), 272(1.895×10^3), 364(5.194×10^2), 667(88)
$[Cu^{II}(hyap\text{-}ppzH)Cl_2]$ (**2**)	MeOH	225(2.237×10^3),270(1.446×10^3), 354(4.443×10^2), 638 (67)
PS-$[Cu^{II}(sal\text{-}ppzH)Cl_2]$ (**3**)	Nujol	225, 273, 364
PS-$[Cu^{II}(hyap\text{-}ppzH)Cl_2]$ (**4**)	Nujol	225, 270, 354, 638

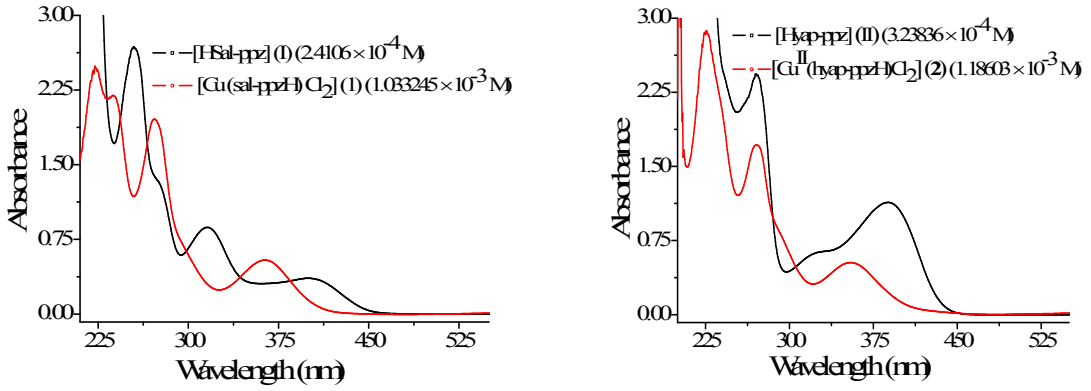

Figure S2: Comparative UV-Vis absorption spectra of ligands with their corresponding copper complexes recorded in methanol.

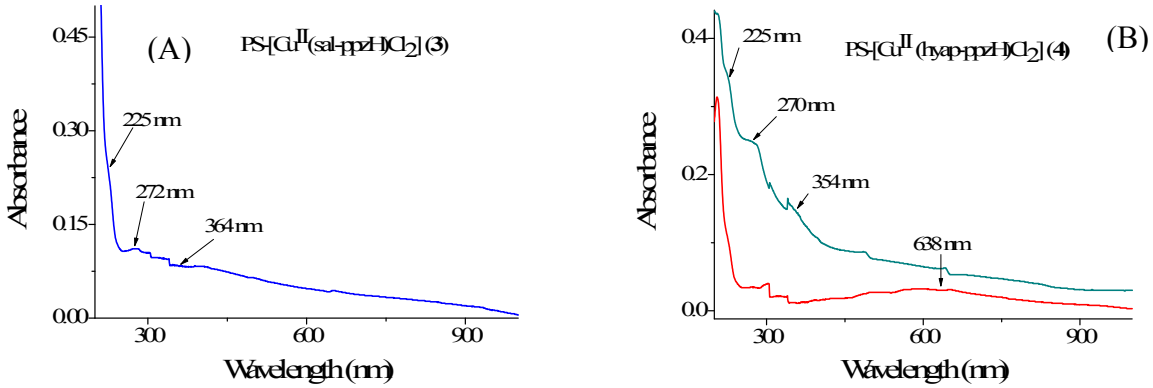

Figure S3: UV-Vis spectra of (A) PS-[Cu^{II}(sal-ppz)Cl] (**3**) and (B) PS-[Cu^{II}(hyap-ppz)Cl] (**4**) in nujol.

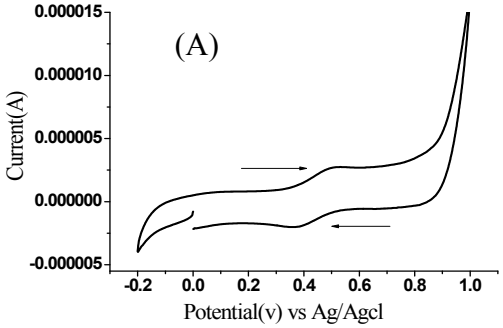

Figure S4: Cyclic Voltagram of complex [Cu^{II}(sal-ppzH)Cl_2] (**1**).

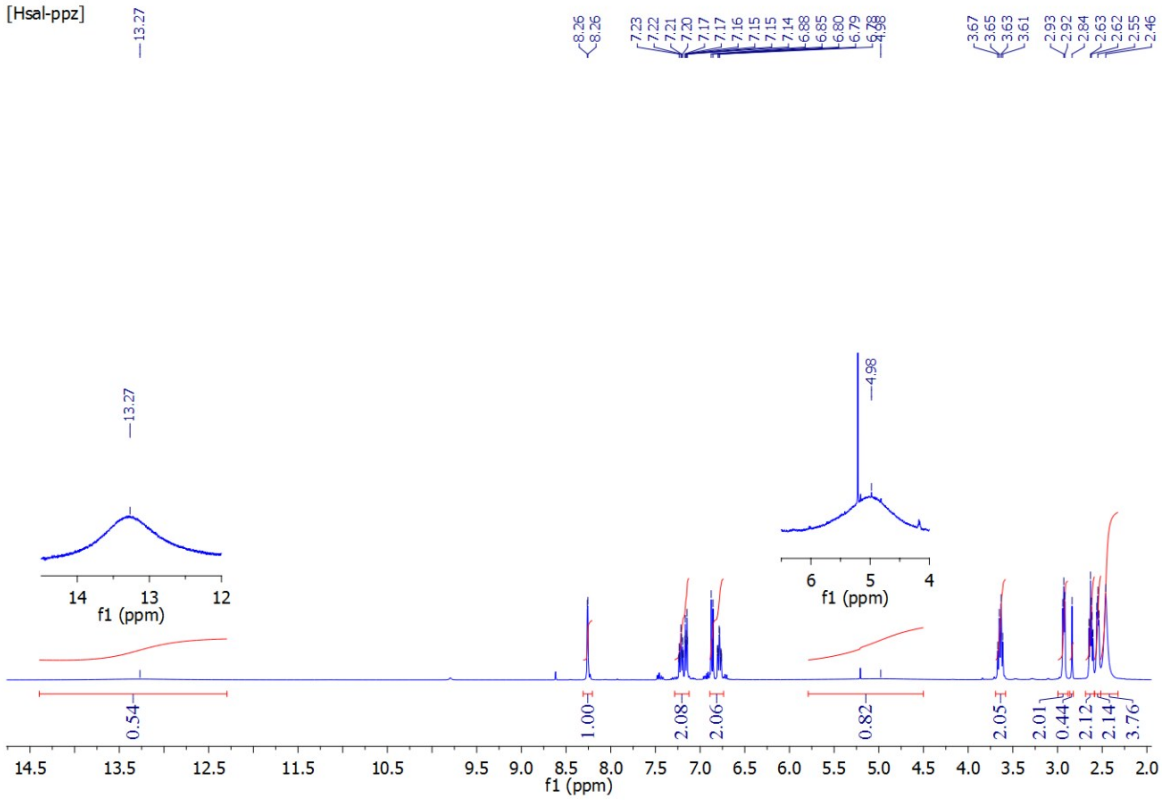

Figure S5: ^{1}H NMR spectra of ligand [Hsal-ppz] recorded in $CDCl_3$.

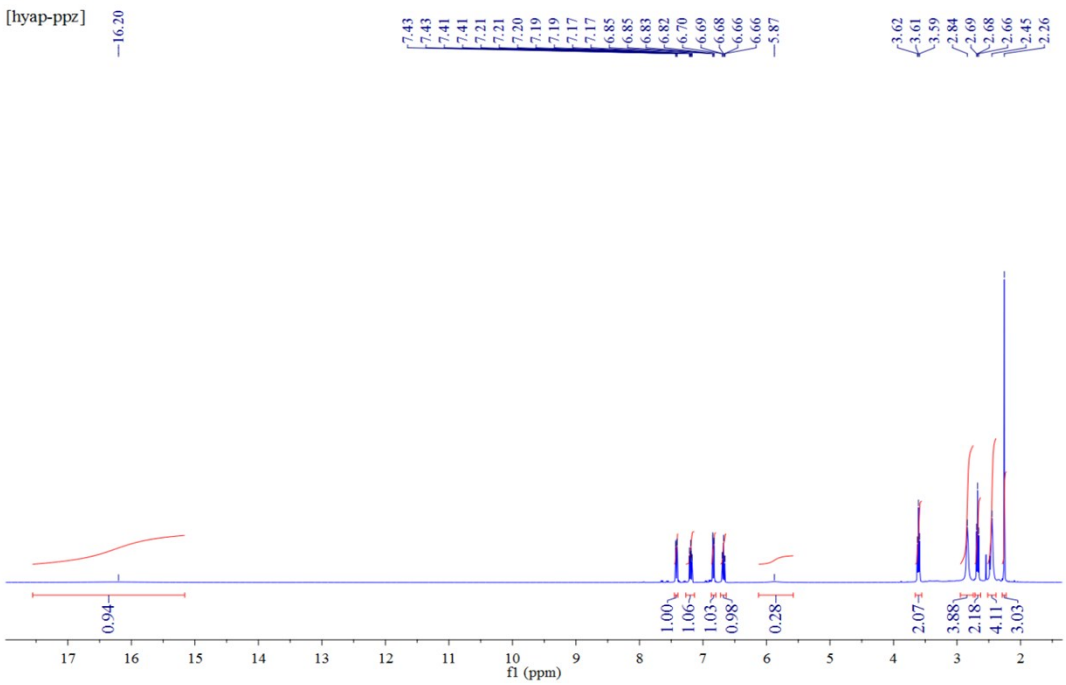

Figure S6: ^{1}H NMR spectra of ligand [Hyap-ppz] recorded in $CDCl_3$.

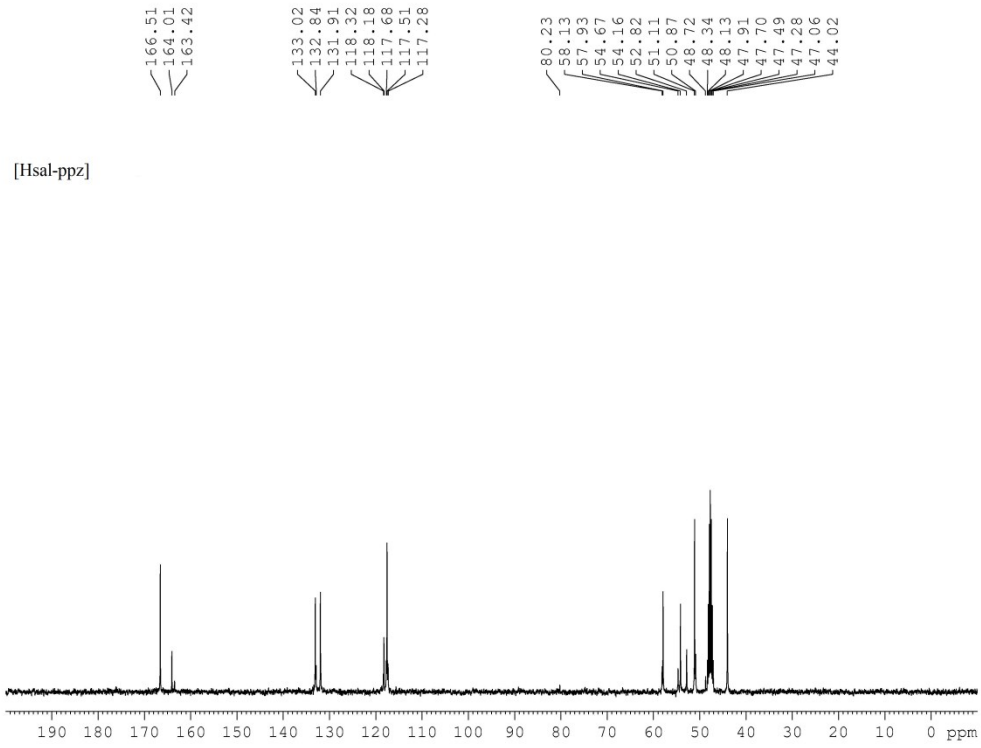

Figure S7:^{13}C NMR spectra of the ligand [Hsal-ppz] **(I).**

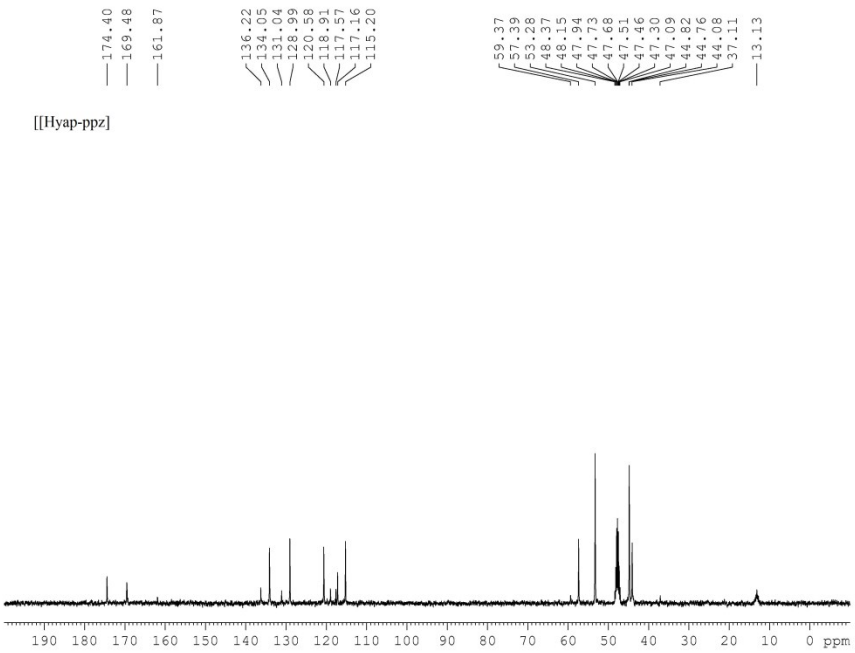

Figure S8: ^{13}C-NMR spectra of the ligand [Hyap-ppz] **(II).**

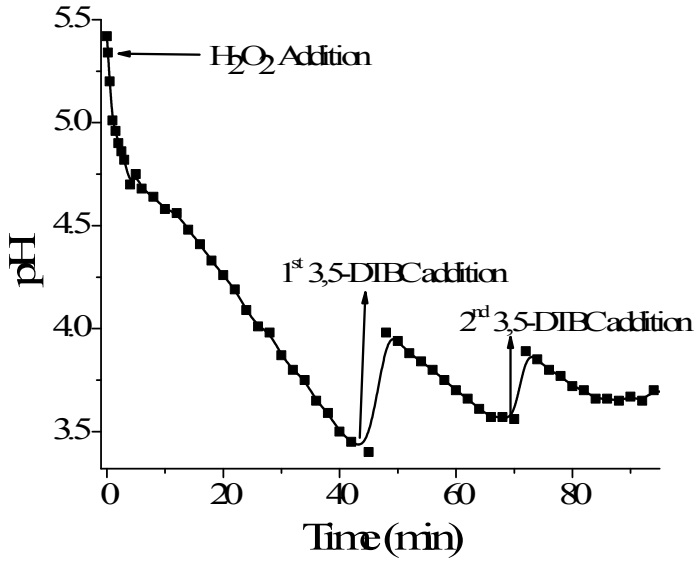

Figure S9: Variation of pH with time for the oxidation of 5 ml 5.698 × 10^{-2} M 3,5-ditert-butyl catechol by 10 ml 1.833×10^{-4} M of **2** in presence of 5 ml 3.96 ×10^{-1} M H_2O_2.

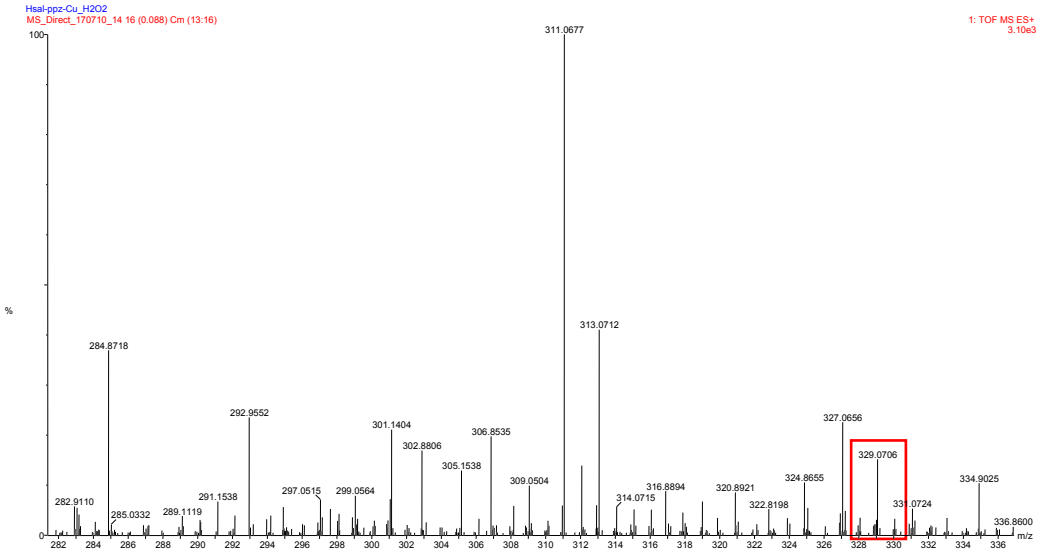

Figure S10: ESI-MS spectra of peroxo Cu^{III} complex $[Cu^{III}(O_2)(sal\text{-}ppzH)]$ (M+H); *m/z* = 329.07

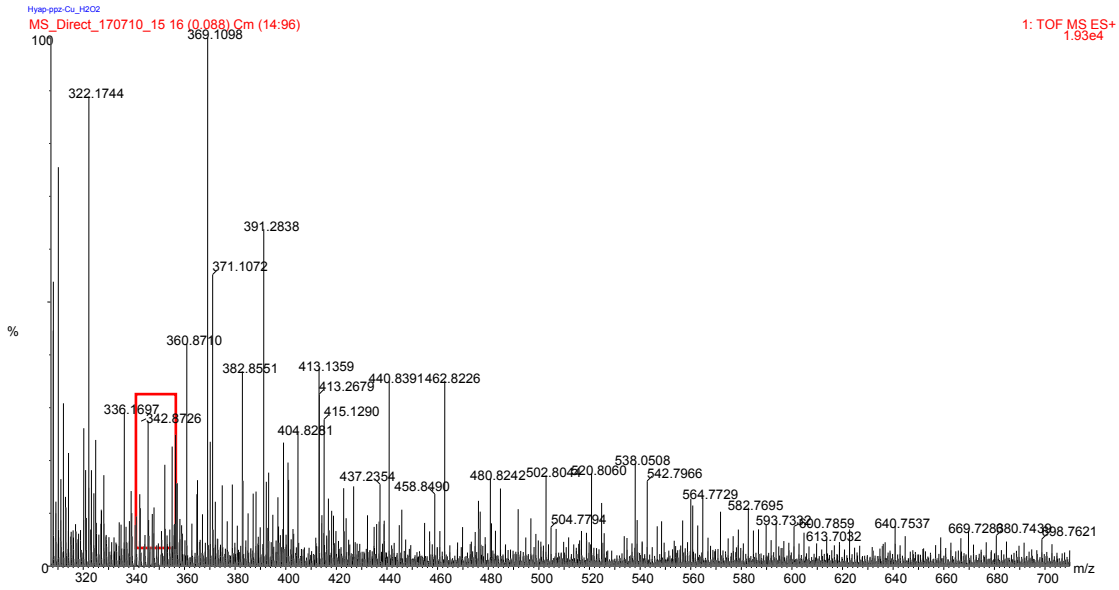

Figure S11: ESI-MS spectra of peroxo Cu^{III} complex $[Cu^{III}(O_2)(hyap\text{-}ppzH)]$ (M+); *m/z* = 342.87

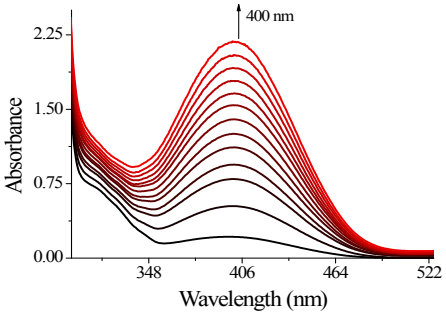

Figure S12: Spectral changes observed during oxidation reaction of 3,5-di-tert-butylcatechol (2.85×10^{-2} M) to corresponding *o*-quinone by **1** (**(**1.83×10^{-5} M) in the presence of 1.0×10^{-1} M H_2O_2 20 ml of methanolic reaction mixture at room temperature for 70 minutes.

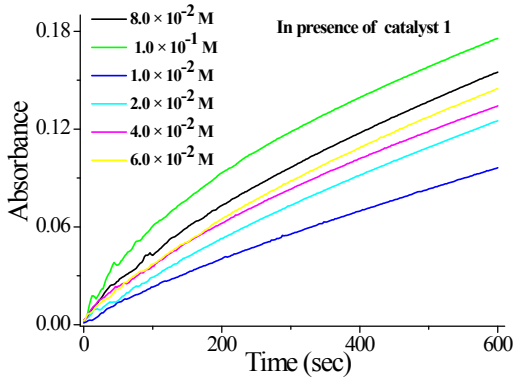

Figure S13: Absorbance vs. time plots for the oxidation of 3,5-DTBC (1×10^{-1} M, 1×10^{-2} M, 2×10^{-2} M, 4×10^{-2} M, 6×10^{-2} M and 8×10^{-2} M) in presence of 1.0×10^{-1} M dilute H_2O_2 with and without catalyst **1** (**(**1×10^{-4} M) for 10 minutes in methanol at room temperature.(Reaction conditions: 1 ml substrate (1×10^{-1} M, 1×10^{-2} M, 2×10^{-2} M, 4×10^{-2} M, 6×10^{-2} M, 8×10^{-2} M) was reacted with 1 ml H_2O_2 (1×10^{-1} M) and 0.5 ml catalyst (1×10^{-4} M) in presence of 1 ml MeOH.)

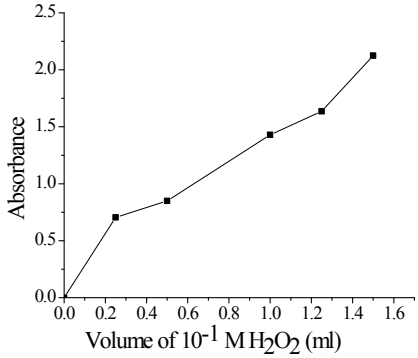

Plot S1: Variation of 3,5-DTBQ absorbance value vs amount of 1.0×10^{-1} M H_2O_2.

Reaction condition: 1.0 ml of 2.85 × 10^{-2} M 3,5-DTBC with 0.5 ml, 1.0 ×10^{-4} M catalyst **2** in presence of 1.0 × 10^{-1} (amount 0.25 ml, 0.50 ml, 1.0 ml and 1.25) M H_2O_2 in a total volume of 3.0 ml of reaction mixture.

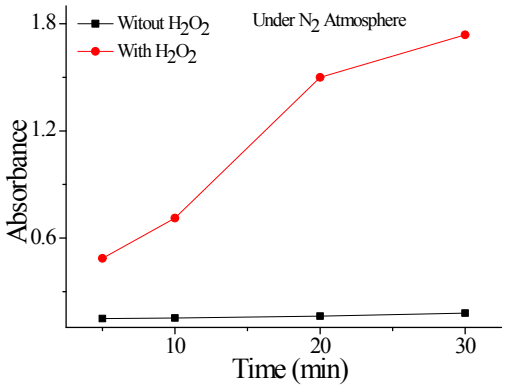

Plot S2: Catalytic oxidation of 3,5-DTBC by catalyst **2** under nitrogen atmosphere with and without H_2O_2. (Reaction condition: 3,5-DTBC 2.85×10^{-2} M, 1.0×10^{-4} M of catalyst **2,** 1.0×10^{-1} M dilute H_2O_2 in a total 20 ml of methanolic reaction mixture at room temperature and pressure.)

Table S4: Oxidative bromination of salicylaldehyde catalyzed by one time and two time recycled catalyst **3** and **4.** % conversion, and % of products obtained after 2 hours of reaction at room temperature and pressure.

SN	Cat. Precursor	catalyst (mg)	Substrate :Oxidant	$HClO_4$ (mmol)	Water (ml)	KBr (mmol)	Conversion %	% of products			
								5-bromosalicylaldehyde	3-bromosalicylaldehyde	3,5-dibromosalicylaldehyde	Unidentified pdts
1	**$CuCl_2.2H_2O$**	0.2973	1:2	20	10	20	84.61	68.77	13.03	2.64	0.162
2	**3***	10	1:2	20	10	20	96.46	75.81	9.57	10.54	0.52
3	**4***	10	1:2	20	10	20	91.54	73.48	14.14	3.74	0.17
4	**3****	10	1:2	20	10	20	88.83	69.86	8.72	9.65	0.60
5	**4****	10	1:2	20	10	20	86.75	69.50	13.53	3.57	0.14

* Shows one time recycle catalyst.

** Shows two time recycle catalyst.

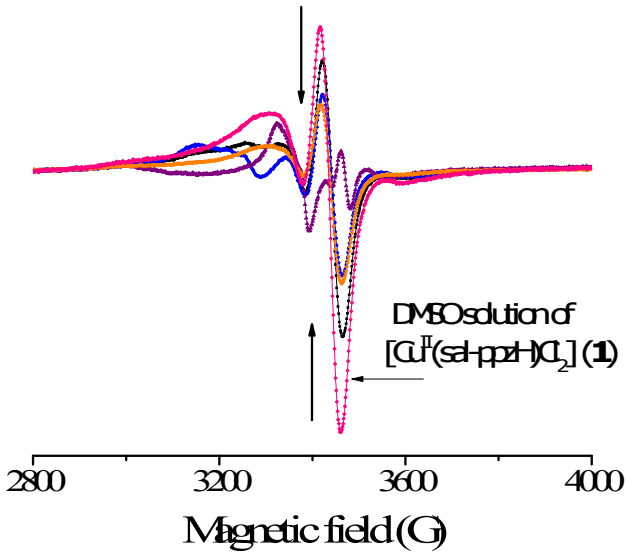

Figure S14: EPR spectra of complex $[Cu^{II}(sal\text{-}ppzH)Cl_2]$ (**1**) were recorded in DMSO. The spectral changes recorded during the successive addition of 1 drop portion of dilute 30 % H_2O_2 into a 20 ml of DMSO solution of **1.**